# 9

# Spectral line transport

## 9.1 Non-LTE

The title non-LTE refers to a method for analyzing the interaction between a gas and the radiation field that accounts for the modification of the excitation and ionization state of the atoms in the gas by the influence of the radiation field. If the radiation field is weak or the density is large, then the occupation probabilities of the atomic states are governed by the dominant collisional processes. In a wide variety of cases the rates of electron–electron and ion–ion collisions, and usually electron–ion collisions as well, are so great that the relaxation of all these species to a single kinetic temperature is essentially complete. So when collisional processes dominate the atomic excitation rates, the result is occupation probabilities that agree with thermodynamic equilibrium, no matter what the radiation intensities may be. This is LTE – local thermodynamic equilibrium. So non-LTE is the other situation. In non-LTE the relaxation of the velocity distributions of the electrons and atoms to a single kinetic temperature is still supposed to be true. But what is *not* true in non-LTE is that collisional processes are generally dominant over the competing radiative processes for populating and depopulating the atomic states.

Non-LTE is a large subject. Good references for non-LTE line transport are Mihalas's *Stellar Atmospheres* (1978), Athay (1972b) and Ivanov (1973). Approximations to the electron-impact excitation rate are discussed by Sobel'man (1979) and by Sampson and Zhang (1992, 1996).

### *9.1.1 Kinetic equations*

As a system for doing calculations, non-LTE consists of solving for the radiation field $I_\nu$ and the set of atomic occupations $N_{ij}$, also often called the "populations." Here $i$ is an index for elements, and $j$ is an index for an energy level belonging to that element. The set of equations that determines these are the transport equation,

which fixes the intensity, and the atomic kinetic equations. The kinetic equations have this generic form:

$$\rho \frac{D(N_{ij}/\rho)}{Dt} = \sum_k \left[ N_{ik}(P_{kj} + C_{kj}) - N_{ij}(P_{jk} + C_{jk}) \right]. \tag{9.1}$$

The $P$s and $C$s are rate coefficients. The $P$s in particular are radiative rates, such as spontaneous and stimulated decay, photoabsorption, and photoionization, and the $C$s are collisional rates, most commonly the ones for inelastic electron collisions. The elastic rates are ignored, since they do not change the level populations (although they count in electron impact line broadening). The electron rates can be expressed as $N_e$ times a collisional rate coefficient, and the latter is a quantity like $\langle v\sigma_{jk} \rangle$, where the brackets indicate an average over the electron Maxwellian distribution of velocities. The radiative rates are combinations of spontaneous downward rates, stimulated downward rates that are written as integrals of appropriate cross sections over the photon flux spectrum, and upward radiative rates that are likewise integrals of photon fluxes times cross sections.

Every rate in (9.1) appears twice, once as a positive term in the equation for the receiving level, and a second time as a negative term in the equation for the originating level. As a result, if all the equations for the levels of all the ions of one element are added up, everything in the sum cancels out. The time derivative on the left turns into $\rho$ times the convective time derivative of the atomic fraction of that element, which vanishes unless there is diffusion (of atoms!) in the fluid.

Of course, time scales vary enormously, but it helps to think about the magnitude of things. A typical flow time scale in the sun or some other star might be around $10^3$ s, or perhaps in some cataclysm as short as 1 s. The lifetime for spontaneous decay in a typical strong spectral line in the optical region is something like $10^{-8}$ s. Radiative recombination lifetimes in stellar atmospheres are on the order of $1/(N_e \alpha_{RR})$ which comes out $10^{-3}$ s if the electron density is $10^{16}$ cm$^{-3}$, a fairly typical value for photospheres. Electron collisional rate coefficients are something like $10^{-8}$ cm$^3$ s$^{-1}$, which makes the collision rate around $10^8$ s$^{-1}$. Some of the photoionization rates, those that involve threshold frequencies in the far-UV, will be vastly smaller than the radiative recombination rates. Thus we see that there is a very large dynamic range of the rate values, from a rate that is perhaps comparable with the flow rate, to processes such as spontaneous bound–bound rates and electron collisions that may be $10^8$ times faster. In other environments the comparisons will differ, but the large dynamic range is a common property. We notice that in this case the rates are (perhaps all?) larger than the flow rate, and that no great error would be committed by dropping the time derivative term. This is often, but not always, a reasonable approximation, called statistical equilibrium.

Let us think for a minute what is entailed in solving a non-LTE problem. We are trying to solve simultaneously (4.23) and (9.1). In both of these the characteristic time for the right-hand side terms may be very short – the light-travel time for the transport equation and the time scale of the fastest rates for the kinetics. A straightforward explicit time differencing of either equation would be subject to a stability condition that restricts the time step to a value smaller than these characteristic times. This is usually prohibitively small. Thus some kind of implicit time differencing must be used, which amounts to solving the steady-state equations for the advanced-time variables, with the time derivative term as a small perturbation. This situation is described by saying that these differential equations (in time) are *stiff*. As the numbers just quoted indicate, the kinetic equations are very stiff indeed, since there may be a factor $10^8$ separating the fastest relaxation time from the time scale on which we would like to integrate. (Those who are familiar with the association between stiffness and the magnitude of the eigenvalues of the Jacobian matrix of the derivatives with respect to the unknowns may want to know that the largest eigenvalue of the rate matrix is comparable with the fastest rate.) Thus we want to consider the worst case of stiffness, which is the steady-state limit, and reality is often close to it.

### 9.1.2 Two-level atom

In order to develop some more of the non-LTE ideas, let us consider the prototype non-LTE problem, which is the two-level atom in a steady state. That is, we restrict ourselves to a single ion, and ignore all but two energy levels, the ground state and an excited state connected to the ground state by a strong line. We use the labels 1 and 2 for the levels, and account for the radiative processes of radiative excitation, spontaneous and stimulated emission, collisional excitation, and collisional deexcitation (superelastic collisions). There is just one rate equation, since the second one is guaranteed to be the same as the first. This is

$$N_1 \left( B_{12} \bar{J}_{12} + N_e C_{12} \right) = N_2 \left( A_{21} + B_{21} \bar{J}_{12} + N_e C_{21} \right). \tag{9.2}$$

The radiative rates have been expressed in terms of the Einstein coefficients. Because the intensity may, indeed will, have some variation within the line bandwidth, the absorption and stimulation emission rates are proportional to a cross-section-weighted angle-averaged intensity:

$$\bar{J}_{12} = \int d\nu \, \phi_{12}(\nu) J_\nu. \tag{9.3}$$

The expressions for the absorptivity and emissivity are as follows (see (8.28), (8.29)):

$$k_\nu = \frac{h\nu}{4\pi}\left(N_1 B_{12} - N_2 B_{21}\right)\phi_{12}(\nu), \tag{9.4}$$

$$j_\nu = \frac{h\nu}{4\pi} N_2 A_{21}\phi_{12}(\nu). \tag{9.5}$$

Notice that we *cannot* assume that the stimulated correction factor is $1 - \exp(-h\nu/kT)$. If we divide the emissivity by the absorptivity we get the line source function,

$$S_\nu = \frac{N_2 A_{21}}{N_1 B_{12} - N_2 B_{21}} = \frac{2h\nu^3/c^2}{N_1 g_2/N_2 g_1 - 1}, \tag{9.6}$$

as we described earlier in (8.21). One thing we notice here is that the shape function $\phi_{12}(\nu)$ has canceled out, and the source function is very nearly independent of frequency. If we inquire a little more deeply into this result, it is a consequence of the assumption that the quantum state of the excited atom has lost any *coherence* it may have acquired in a photoexcitation, and has the same random phase that it would have if it were collisionally excited, for example. Reality is more complicated. If the probability of a radiative decay vastly exceeds the probability of any collisional process, then the coherence is *not* lost, which means that the frequency profile of the emitted radiation will contain traces of the spectral distribution of the radiation that produced the excitation. This situation is called *partial redistribution* and will be discussed in the next section. We note that scattering of a photon in the wing of a resonance line takes two forms, which correspond to the two possibilities for coherence. If the coherence is retained, then the emitted photon has essentially the same frequency as the absorbed photon, and this process is called *Rayleigh scattering*. When the coherence is lost, the emitted photon frequency is near line center, and the process is called *resonance fluorescence*. When the incoming photon's frequency is quite far in the wing, the Rayleigh scattering process predominates. A general term for scattering in which the coherence is lost is *complete redistribution*, and this is what we shall assume for the present.

The rate equation can be solved for $N_1/N_2$ which is then substituted into the formula for $S_\nu$. Before doing so we note that the collisional rate coefficients must themselves be consistent with LTE. The upward and downward electron-collision rate coefficients are determined by the velocity distribution of the electrons, which we assume to be Maxwellian at the temperature $T$. The upward and downward collision rates would then balance if the atomic populations obeyed the Boltzmann

excitation formula at the same temperature. This leads to

$$C_{12} = \frac{g_2}{g_1} e^{-h\nu_0/kT} C_{21} \tag{9.7}$$

in view of the Boltzmann excitation formula, since $h\nu_0$ is the excitation energy. Performing the substitutions leads to this expression when the radiative rates are also included:

$$S_\nu = (1-\epsilon)\bar{J}_{12} + \epsilon B_\nu, \tag{9.8}$$

with

$$\frac{\epsilon}{1-\epsilon} = \frac{N_e C_{21}}{A_{21}} \left[1 - \exp(-h\nu_0/kT)\right]. \tag{9.9}$$

The formula (9.8) strongly resembles the scattering source function considered in Milne's second problem (see Section 5.5), and $1-\epsilon$ is analogous to the scattering albedo. We can regard the line scattering event in this way. When a photoexcitation occurs, the excited atom can decay in two ways. Either it decays radiatively, producing another photon, or it decays by a superelastic collision, in which case we say that the excitation has been quenched. In the first case we can say that the photon has been reborn, and begins its next flight, while in the second case we say that the collision has killed the photon. The branching ratio for reemission is the albedo. Apart from the factor $1 - \exp(-h\nu_0/kT)$ this is simply given by the ratio of the $A$ value to the sum of the $A$ value and the collisional deexcitation rate. To repeat: this is not scattering in the sense of Thomson or even Rayleigh scattering, since in those cases the amplitude for emission combines coherently with the amplitude for absorption. Here we assume that the excited atom lingers a while, so that its phase is scrambled before reemission. However, in the far wings of the line, the uncertainty principle for time vs energy requires that the emission occur promptly, which makes the process coherent. Thus line scattering as we describe it here goes over into Rayleigh scattering in the far wings of the line. Complete redistribution is inappropriate in that case.

There is a useful approximate relation between $C_{21}$ and $A_{21}$ due to Van Regemorter (1962) which is found when the process of electron impact excitation is treated in a large-$r$ dipole approximation. It is

$$\frac{C_{21}}{A_{21}} \approx \frac{0.2\lambda^3 g}{\sqrt{T/10^4\,\mathrm{K}}}, \tag{9.10}$$

in which $g$ is formally the same as the free–free Gaunt factor $\bar{g}_{III}(\nu_0)$, but is better regarded as a fitting constant. Comparing (9.10) with accurate electron excitation calculations suggests that $g \approx 0.2$ is a good choice for collisions with positive ions, except that transitions between states of the same principal quantum number

$n$ require a larger value, more like unity. Using the Van Regemorter formula gives this simple result for $\epsilon$:

$$\frac{\epsilon}{1-\epsilon} \approx \frac{0.2 N_e \lambda^3 g \left[1 - \exp(-h\nu_0/kT)\right]}{\sqrt{T/10^4\,\mathrm{K}}}. \tag{9.11}$$

The wavelength $\lambda$ that appears here is the wavelength of the spectral line being considered. Just so we can appreciate the order of magnitudes involved, we suppose that $T$ is $10^4$ K and the line is in the visible part of the spectrum, so $\lambda \approx 5000$ Å. The result for $\epsilon/(1-\epsilon)$ is $N_e/4 \times 10^{13}\,\mathrm{cm}^{-3}$. The place in the solar atmosphere where the electron density is $4 \times 10^{13}$ is near the photosphere; the electron density there is much smaller than the value $10^{16}$ mentioned earlier since the degree of ionization is low. In the atmosphere of a hot star this electron density comes at approximately $\tau = 10^{-2}$. The resonance lines we are considering are formed higher in the atmosphere than either of these estimates, and so we generally expect $\epsilon$ to be small.

We will describe the solution of the simplest problem of resonance line transfer, namely finding the source function and the emergent spectrum when the temperature and $\epsilon$ are uniform in a half-space. We need to introduce an optical depth scale that describes the line as a whole in a meaningful way, and the first step toward this is to introduce a frequency scale measured in units of the Doppler width from the center of the line. Here the Doppler width is $\sqrt{2}$ times the standard deviation of the Gaussian profile, $\Delta\nu_D = \nu\sqrt{2kT/Mc^2}$. Our scaled frequency is

$$x = \frac{\nu - \nu_0}{\Delta\nu_D}. \tag{9.12}$$

We then use a cross section profile function that is normalized on the $x$ scale:

$$\int_{-\infty}^{\infty} dx\, \phi(x) = 1. \tag{9.13}$$

Next we define the optical depth scale $\tau$, without a frequency suffix, so that $\tau_\nu = \tau\phi(x)$. This means that $\tau$ is calculated from

$$d\tau = \frac{h\nu_0}{4\pi\,\Delta\nu_D}(N_1 B_{12} - N_2 B_{21})dz. \tag{9.14}$$

For simplicity we assume that $\phi(x)$ is independent of depth, which is reasonable for a constant temperature atmosphere.

Now we can obtain $J_\nu$ from (5.25) applied frequency-by-frequency,

$$J_\nu(\tau) = \frac{1}{2}\int_0^\infty \phi(x) d\tau'\, E_1(\phi(x)|\tau' - \tau|) S(\tau'). \tag{9.15}$$

Next we multiply by $\phi(x)$ and integrate over $x$ to obtain $\bar{J}$:

$$\bar{J}(\tau) = \int_0^\infty d\tau\, K_1(\tau' - \tau) S(\tau'), \tag{9.16}$$

where $K_1(\tau)$ is a new kernel function defined by

$$K_1(\tau) = \frac{1}{2} \int_{-\infty}^{\infty} dx\, \phi^2(x) E_1(\phi(x)|\tau|). \tag{9.17}$$

The $K_1$ function is normalized to unity, as can easily be shown by integrating over $\tau$ under the integral over $x$, then using the normalization of $\phi$. But this function is very different in character from those kernels, like $E_1(\tau)$, that fall off exponentially at large $\tau$. In fact, in the important Doppler broadening case $K_1$ falls off only as $1/\tau^2$ for large $\tau$. That means that *the mean free path for line scattering is infinite*. This is a major difference between line scattering and Thomson scattering, say. If a photon does $10^4$ Thomson scatterings, then its net displacement is about $\Delta\tau = 100$, since each flight represents a rms step of 1 in $\tau$, and the flights add in the square. Line transport does not work that way. On each flight in a line transfer problem the photon chooses a frequency by sampling the distribution $\phi(x)$, then it goes a distance of order $1/\phi(x)$ in $\tau$. What happens after many flights is actually this: *the net displacement is contributed almost entirely by the one flight for which the sampled frequency was farthest from line center*. Line photons do not diffuse when there is complete frequency redistribution.

Consider those $10^4$ line scatterings again and assume the line profile is Doppler, $\phi(x) = \exp(-x^2)/\sqrt{\pi}$. The largest frequency $x$ of that many samples will be about the value for which the integral of the tail of $\phi$ from $x$ to $\infty$ is around $10^{-4}$. But the integral is approximately $\phi(x)/2x$. Thus the value of $\phi$ for this $x$ is roughly the same as the tail probability, namely $10^{-4}$, so the mean free path *at this frequency* is $10^4$ in $\tau$ units, and that is how far the photon goes on that one flight. So for line scattering with a Doppler line profile, the net displacement after a large number $N$ of scatterings is of order $N$, not $\sqrt{N}$ as it would be in the usual random walk.

The integral with respect to $\tau$ of the $K_1$ function defines the $K_2$ function:

$$K_2(\tau) = 2\int_\tau^\infty d\tau'\, K_1(\tau') = \int_{-\infty}^{\infty} dx\, \phi(x) E_2(\phi(x)\tau) \qquad \tau > 0. \tag{9.18}$$

If, in (9.16), $S(\tau')$ is evaluated at $\tau' = \tau$ and taken out of the integral, the result is

$$\bar{J}(\tau) \approx [1 - p_{\rm esc}(\tau)] S(\tau), \tag{9.19}$$

in which the two-sided escape probability is now given by

$$p_{\rm esc}(\tau) = \frac{1}{2}K_2(\tau). \tag{9.20}$$

This is analogous to the monochromatic equation (5.24) discussed earlier, except that now we are considering the escape of line photons from the medium when the frequency can change randomly at each scattering. The nature of the kernels $K_1(\tau)$ and $K_2(\tau)$ is all-important in setting the qualitative nature of the escape of line radiation. The different shapes of line profile $\phi(x)$ lead to different kernel behavior for large $\tau$, as shown by Avrett and Hummer (1965). For $K_1(\tau)$:

$$K_1(\tau) \sim \begin{cases} \dfrac{1}{4\tau^2\sqrt{\ln(\tau/\sqrt{\pi})}} & \text{Doppler} \\ \dfrac{\sqrt{a}}{6\tau^{3/2}} & \text{Voigt, } a\tau \gg 1. \\ \dfrac{1}{6\tau^{3/2}} & \text{Lorentzian} \end{cases} \tag{9.21}$$

For $K_2(\tau)$:

$$K_2(\tau) \sim \begin{cases} \dfrac{1}{2\tau\sqrt{\ln(\tau/\sqrt{\pi})}} & \text{Doppler} \\ \dfrac{2\sqrt{a}}{3\sqrt{\tau}} & \text{Voigt, } a\tau \gg 1. \\ \dfrac{2}{3\sqrt{\tau}} & \text{Lorentzian} \end{cases} \tag{9.22}$$

The Milne equation to be solved for the source function for the constant-temperature half-space problem is the following:

$$S(\tau) = \epsilon B_\nu + (1-\epsilon)\int_0^\infty d\tau' K_1(\tau'-\tau)S(\tau'). \tag{9.23}$$

We will skip the analytical solution methods, which can just be copied over from the single-frequency or gray case, and go to the results. The value of $S$ at the surface $\tau = 0$ is $\sqrt{\epsilon}B_\nu$, an exact result. Then $S$ rises from that value with increasing $\tau$ more or less as $\tau^{1/2}$ and eventually reaches $B_\nu$ when $\tau$ is approximately the thermalization depth. The thermalization depth can be found from the root of a transcendental equation similar to (5.42). It also comes from a physical argument. When $\epsilon$ is a small number, the photon will survive about $N = 1/\epsilon$ flights before being destroyed. The thermalization depth is about equal to the net distance the photon will go in that many flights, which as we have seen is about $\Delta\tau = N$. Therefore the thermalization depth is approximately $1/\epsilon$ on the $\tau$ scale for the

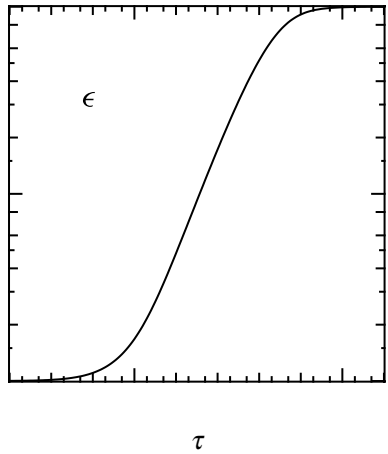


Fig. 9.1 Source function $S$ of a line in a semi-infinite isothermal atmosphere formed with complete redistribution over a Doppler profile, with $\epsilon = 10^{-4}$, in units of Planck function $B$ vs optical depth scale of (9.14).

case of Doppler broadening. This does vary with the shape of the line profile, so for example, for a Lorentzian profile the thermalization depth is roughly $1/\epsilon^2$. A more precise definition of the thermalization depth $\Lambda$ that is consistent with this argument is given by the statement

$$K_2\left(\frac{1}{2}\Lambda\right) = \epsilon. \tag{9.24}$$

When scattering is quite dominant, so $\epsilon$ is very small, the relations for the thermalization depth with the various profiles are

$$\Lambda \sim \begin{cases} \dfrac{1}{\epsilon\sqrt{-\ln(\sqrt{\pi}\epsilon)}} & \text{Doppler} \\ \dfrac{8}{9}\dfrac{a}{\epsilon^2} & \text{Voigt, } a \gg \epsilon. \\ \dfrac{8}{9}\dfrac{1}{\epsilon^2} & \text{Lorentzian} \end{cases} \tag{9.25}$$

The source function for the constant-temperature half-space with Doppler broadening and for $\epsilon = 10^{-4}$ is illustrated in Figure 9.1.

The shape of the line in the spectrum of the emergent flux follows from an application of the ordinary Eddington–Barbier relation. Thus at line center the flux is about $\pi$ times the surface source function, or $\pi\sqrt{\epsilon}B_\nu$, then away from line center it rises in proportion to $1/\phi(x) \propto \exp(x^2)$ until it reaches the level of $\pi B_\nu$ at $x \approx \sqrt{-\log(\epsilon)/2}$. This gives a trough-shaped profile with quite a black center

and steep edges. When the temperature distribution is high at $\tau = 0$, goes through a broad minimum at some large value of $\tau$, and increases again at yet larger $\tau$, which is a rough picture of the solar transition region, chromosphere, and photosphere, the same kind of argument can be used to sketch the emergent spectrum. If the value of $\tau$ at the temperature minimum is greater than the thermalization depth, then the source function will be small at the surface, owing to $\sqrt{\epsilon}$, then rise inward until at the thermalization depth it meets the Planck function, which has been declining over this range. The source function goes through a maximum at this point. Going further inward, the source function follows the Planck function down to the minimum, then up again going on down through the photosphere. This shape of the source function vs depth maps into the shape of the emergent flux vs frequency: it is very small at line center, increases away from the center, goes through a maximum at the displacement from center where the mean free path corresponds to the thermalization depth, then drops again farther from line center, goes through a very broad minimum, and finally rises toward the continuum when the mean free path reaches all the way to the photosphere. This is the picture of the Ca II H and K lines and the Mg II h and k lines in the solar spectrum.

### *9.1.3 Ivanov's approximation*

Owing to the nondiffusive character of line transport with complete frequency redistribution, a good approximation for the spatial variation of the source function in a finite or semi-infinite medium with slab symmetry is not simple to obtain. Sobolev's Russian school, and notably V. V. Ivanov, have been successful at doing this. In an analysis that is too long to reproduce here, Ivanov (1973) obtains this approximate solution of the finite slab problem with a uniform Planck function $B_\nu$:

$$S \approx \frac{\epsilon B_\nu}{\sqrt{[\epsilon + (1-\epsilon)K_2(\tau)][\epsilon + (1-\epsilon)K_2(\tau_0 - \tau)]}}, \tag{9.26}$$

where $\tau$ is the optical depth measured from one face of the slab and $\tau_0$ is the optical thickness of the slab. $K_2(\tau)$ is the kernel given in (9.18). It has the limits $K_2(\tau) \to 1$ for $\tau \to 0$, and $K_2(\tau) \to 0$ for $\tau \to \infty$. Equation (9.26) has all the right limits: $S \sim \epsilon B_\nu$ when $\tau_0 \to 0$, $S \sim B_\nu$ for $\tau$, $\tau_0 - \tau \to \infty$, and $S(0) = \sqrt{\epsilon} B_\nu$ for $\tau = 0$ and $\tau_0 \to \infty$. In Section 8.11 of Ivanov (1973) the accuracy of (9.26) is computed, and it is always within a factor 2 and often within 20%.

### *9.1.4 Multilevel atom*

The non-LTE problems of practical importance involve more than two levels, indeed they may involve a great many levels. An important stepping-stone to solving

such multilevel problems is to treat the spectral lines one at a time, in each case accounting for the response of the populations of the upper and lower levels of this one line to changes in its own radiation field, but omitting the changes that may occur in the other levels. This is the *equivalent two-level atom* method (ETLA) that has been developed by Avrett (1965), Avrett and Kalkofen (1968), Avrett and Loeser (1987), and others. Let the line in question be formed in the transition between lower level $\ell$ and upper level $u$. The source function expression (9.6) becomes for this line

$$S_\nu = \frac{2h\nu^3}{c^2} \frac{1}{(b_\ell/b_u)\exp(h\nu/kT) - 1}, \tag{9.27}$$

in which $b_\ell$ and $b_u$ are the *departure coefficients* of the level populations from LTE:

$$b_n \equiv \frac{N_n}{N_n^*}, \tag{9.28}$$

in which the quantity $N_n^*$ is the population of level $n$ calculated on the basis of thermodynamic equilibrium at the local electron temperature. One technical point to note about (9.27) is that $\nu$ need *not* be treated as constant across the line profile. In fact, a more careful analysis of the absorptivity and emissivity profiles shows that on the assumption of complete frequency redistribution in the line scattering, the frequency dependences of absorption, spontaneous emission, and stimulated emission are related in just the way needed for (9.27). This is discussed by Castor, Dykema, and Klein (1992). That reference will be used for the following discussion.

The ratio $b_\ell/b_u$ can be found by solving the kinetic equations for the two populations $N_\ell$ and $N_u$, assuming the remaining populations are given. The full kinetic equations for the two levels $\ell$ and $u$, in the steady-state case with $D(N_n/\rho)/Dt = 0$, become

$$\begin{aligned} (P_{\ell u} + C_{\ell u} + a_1)N_\ell - (P_{u\ell} + C_{u\ell})N_u &= a_2, \\ -(P_{\ell u} + C_{\ell u})N_\ell + (P_{u\ell} + C_{u\ell} + a_3)N_u &= a_4. \end{aligned} \tag{9.29}$$

The terms including $N_\ell$ and $N_u$ are put on the left-hand sides of these equations, and the remaining terms are put on the right. The rate coefficients connecting levels $\ell$ and $u$ are broken into their radiative and collisional parts, $P$ and $C$. The photoexcitation rate is given by

$$P_{\ell u} = \int_0^\infty \frac{4\pi\sigma_\nu}{h\nu} J_\nu \, d\nu, \tag{9.30}$$

and the photo deexcitation rate is

$$P_{u\ell} = \left(\frac{N_\ell}{N_u}\right)^* \int_0^\infty \frac{4\pi\sigma_\nu}{h\nu}\left(\frac{2h\nu^3}{c^2} + J_\nu\right)\exp\left(-\frac{h\nu}{kT_e}\right)d\nu, \tag{9.31}$$

in which $T_e$ is the local electron temperature and $(N_\ell/N_u)^*$ is the LTE population ratio at that temperature. The photoabsorption cross section $\sigma_\nu$ can be put back in terms of the oscillator strength and the line profile function, if desired. The quantities $a_1$–$a_4$ are terms representing rates from $\ell$ or $u$ to other levels ($a_1$ and $a_3$) and terms representing population flow into levels $\ell$ or $u$ from other levels ($a_2$ and $a_4$). They are given by

$$\begin{aligned} a_1 &= \sum_{i\neq\ell,u} R_{\ell i}, \qquad a_2 = \sum_{i\neq\ell,u} R_{i\ell}N_i, \\ a_3 &= \sum_{i\neq\ell,u} R_{ui}, \qquad a_4 = \sum_{i\neq\ell,u} R_{iu}N_i; \end{aligned} \tag{9.32}$$

The rate coefficients $R$ represent the sum of radiative and collisional coefficients.

The two equations (9.29) are readily solved for $N_\ell$ and $N_u$, and the ratio of these gives the source function:

$$S_\nu = \gamma_\nu P_{\ell u} + \epsilon_\nu, \tag{9.33}$$

in which the coefficients $\gamma_\nu$ and $\epsilon_\nu$ depend on the rates:

$$\gamma_\nu = \frac{2h\nu^3/c^2}{(c_2+c_4)\exp(h\nu/kT_e) - c_1 - c_3}, \tag{9.34}$$

$$\epsilon_\nu = \frac{2h\nu^3}{c^2}\frac{c_3}{(c_2+c_4)\exp(h\nu/kT_e) - c_1 - c_3}, \tag{9.35}$$

and, furthermore, the coefficients $c_1$–$c_4$ are given by

$$\begin{aligned} c_1 &= P_{\ell u}, \qquad c_2 = P_{u\ell}\left(\frac{N_u}{N_\ell}\right)^*, \\ c_3 &= C_{\ell u} + \frac{a_1 a_4}{a_2+a_4}, \qquad c_4 = \left(C_{u\ell} + \frac{a_2 a_3}{a_2+a_4}\right)\left(\frac{N_u}{N_\ell}\right)^*. \end{aligned} \tag{9.36}$$

These expressions do not require that the line be narrow, so that $\nu \approx$ constant could be assumed; thus they work equally well for photoionization continua. A complexity is that (9.33) is nonlinear in the radiation intensity $J_\nu$ in the line because of the appearance of $P_{\ell u}$ and $P_{u\ell}$ in the denominators of (9.34) and (9.35). For narrow spectral lines the exponential factor in the integral defining $P_{u\ell}$ can be taken out of the integral and evaluated at line center, so that when $\gamma_\nu$ and $\epsilon_\nu$ are calculated

at line center the stimulated emission part of $c_2 \exp(h\nu/kT_e)$ precisely cancels $c_1$, and this nonlinearity disappears.

Continuing with the narrow-line approximation, we simplify (9.33) by putting the cross section in terms of the Einstein $A$ coefficient and the profile function, in which we make use of (8.23) and (8.27). We finally get

$$S_\nu = \frac{\bar{J} + \epsilon' B_\nu + \eta B^*}{1 + \epsilon' + \eta}, \tag{9.37}$$

with the definitions

$$\epsilon' = \frac{C_{u\ell}[1 - \exp(-h\nu/kT_e)]}{A_{u\ell}}, \tag{9.38}$$

$$\eta = \frac{a_2 a_3 - (g_\ell/g_u) a_1 a_4}{A_{u\ell}(a_2 + a_4)}, \tag{9.39}$$

$$B^* = \frac{2h\nu^3/c^2}{g_u a_2 a_3/(g_l a_1 a_4) - 1}. \tag{9.40}$$

This form of the source function expression differs from the simple two-level form (9.8) by the presence of the indirect terms $\eta$ and $\eta B^*$ that involve coupling to other levels. The value of $\eta$ can be interpreted as a quenching rate, involving an upper-level atom going to some other level and then returning to the lower level, corrected in some way for stimulated emission, in terms of the direct spontaneous decay rate. This indirect process effectively destroys a line photon, and thus it contributes to the denominator in the source function expression. The numerator term $\eta B^*$ involves the reverse indirect process: a lower-level atom is taken to some other level, from which it returns to the upper level, thus effectively creating a line photon.

When the transfer equation has been solved for this particular line, the results for the radiative rates $P_{\ell u}$ and $P_{u\ell}$ are saved for the next solution of the kinetic equations to yield the level populations. Avrett and Loeser (1987) and others parameterize the rates in terms of a quantity $z$ that is variously called the Net Radiative Bracket (Thomas, 1960), escape factor (Athay, 1972b) or flux divergence coefficient (Canfield and Puetter, 1981). This is defined for narrow lines by

$$z \equiv 1 - \frac{\bar{J}}{S} = \epsilon' \left( \frac{B_\nu}{S} - 1 \right) + \eta \left( \frac{B^*}{S} - 1 \right). \tag{9.41}$$

The second form follows using (9.37). If we compare (9.41) with (9.19) for the escape probability approximation, we see that the Net Radiative Bracket is the accurate quantity that the escape probability approximates. The net radiative rate for transitions from level $u$ to level $\ell$ is easily expressed, for narrow lines, in terms

of the Net Radiative Bracket as follows:

$$N_u P_{u\ell} - N_\ell P_{\ell u} = N_u A_{u\ell} z, \tag{9.42}$$

so that if the rates $P_{\ell u}$ and $P_{u\ell}$ are replaced by $P_{\ell u}^{\text{eff}} = 0$ and $P_{u\ell}^{\text{eff}} = A_{u\ell} z$, the self-consistent solution for the level populations will be unchanged. This replacement has been found to significantly improve the convergence of the ETLA iteration method. Castor, Dykema, and Klein (1992) provide the relations that can be used to compute the Net Radiative Brackets and the effective rates without making the narrow-line approximation, and in that paper the ETLA formulation was applied to both lines and continua.

Equation (9.37) has been the basis of much of the discussion of line formation in the solar chromosphere by Thomas, Athay, Jefferies, and coworkers (see Thomas and Athay (1961)). They have found, for instance, that the $\epsilon'$ term dominates for the H and K resonance lines of Ca II, while the $\eta$ term is more important for the hydrogen Balmer lines, with the result that the temperature rise in the chromosphere produces emission features in the profiles of H and K, but not in the Balmer profiles. The hydrogen Lyman lines are found to be similar to the Ca II lines in this respect, and in fact are strongly in emission.

The ETLA method is used by Avrett and coworkers, and was also used by Castor *et al*. (1992), but it is by no means the only method for treating multilevel non-LTE problems.

The complete linearization method of Auer and Mihalas (1969) has been used on a large scale to solve non-LTE problems with tens or more of atomic levels. A good review of the linearization method(s) has been given by Auer (1984). The basic structure of the original (Auer and Mihalas, 1969) linearization method is as follows. The Feautrier variable $j(\mu)$ (see Section 5.6) is used to represent the radiation field at a set of angle and frequency points, with $NJ$ angle-frequency pairs in all. The level populations $N_1, N_2, \ldots, N_{NL}$ are another part of the set of unknowns. The total density or pressure and the temperature may be added to the list if the constraints of hydrostatic equilibrium and radiative energy balance are imposed. All these variables are specified on a mesh of space points, $z_1, z_2, \ldots, z_{ND}$. If $X_i$ represents the unknowns at space point $i$: $X_i = (j_1, \ldots, j_{NJ}, N_1, \ldots, N_{NL}, N_{\text{tot}}, T)$, then the full solution vector is $\mathbf{X} = (X_1, X_2, \ldots, X_{ND})$. Thus there are $ND(NJ + NL + 2)$ unknowns. There are also this many equations to determine them. There is a Feautrier equation (5.49) corresponding to each $j$ and a population kinetic equation corresponding to each $N$. At the spatial boundaries the Feautrier equation is not used; rather, there is a relation between $j$ on the boundary and the $j$ at the next point away from the boundary that is derived from the relation between $h$ and $j$ at the boundary which expresses the constraint of a certain (or zero) incoming intensity, or reflection symmetry. There

are also not $N_{NL}$ independent kinetic equations in the steady-state case, since the sum of all $N_{NL}$ equations identically vanishes in this case. One of the equations must be replaced by the condition of number conservation, $\sum N_\ell = N_{\rm tot}$. If $N_{\rm tot}$ is not one of the unknowns, then it must be given as data.

In the complete linearization method this system of equations is just treated as the large nonlinear system it is, and the method of solution is the Newton–Raphson method. That is, if $\mathbf{F}(\mathbf{X}) = 0$ represents the set of equations and $\mathbf{X}$ is the solution vector just described, then one step of the iteration process is described by

$$\mathbf{X}^{n+1} = \mathbf{X}^n - \left[\frac{\partial \mathbf{F}(\mathbf{X}^n)}{\partial \mathbf{X}}\right]^{-1} \mathbf{F}(\mathbf{X}^n). \tag{9.43}$$

There are the usual problems with Newton–Raphson, and these arise here. A reasonable first guess is required, or else the iterates quickly diverge. And if the correction to $\mathbf{X}^n$ that is calculated by solving the linear system has excessively large values for some components, such that the estimates of these components of $\mathbf{X}^{n+1}$ would be in unphysical ranges, then all of the corrections may need to be scaled down to keep the new unknowns in the physical range. The special problem in the complete linearization method is the sheer size of the system of equations (9.43). For example, if $NJ = 4000$, $NL = 50$ and $ND = 100$, then the system size is $405\,200 \times 405\,200$. This would be called a small problem. Quite obviously one does not simply apply Gaussian elimination to this system. If it were possible to do so within the constraints of memory, the cost would be of order $ND^3(NJ + NL + 2)^3 \approx 7 \times 10^{16}$ operations. Partitioning methods are applied instead. More recently, iterative methods such as preconditioned Newton–Krylov have been used, but for the present discussion we will stick to direct solution methods. Iterative methods will be considered in Section 11.11.

The partitioning employed by Auer and Mihalas makes use of the sparsity of the Jacobian matrix $\partial \mathbf{F}(\mathbf{X}^n)/\partial \mathbf{X}$ as follows. The Feautrier equations couple the intensity at a given space point to its nearest-neighbor space points on each side. The population kinetics equations and the constraint equations are local in space. Thus the large matrix has a block tri-diagonal structure in which the blocks contain all the unknowns at a single space point. That is, the block size is $NJ + NL + 2$ square. The larger system is solved using the standard recursion scheme for tri-diagonal matrices, except applied here to the blocks. Each step of the (forward) recursion requires of order $(NJ + NL + 2)^3$ operations, and there are $ND$ steps, so the total cost is $ND(NJ + NL + 2)^3$ operations, which is $ND^2$ times fewer than the ignorant elimination.

Rybicki (1971) suggest a different partitioning of the matrix, which, as Auer (1984) points out, makes the method scale in the same way as radiative

transfer solutions using numerical quadrature of the Milne equation (5.37). The idea is simple: the values of $j(\mu, \nu)$ at various angles and frequencies enter the kinetic equations only in the combinations that define $\bar{J}$, namely $\int d\mu \int d\nu\, \phi(\nu) j(\mu, \nu)$. But each $j(\mu, \nu)$ can be found by solving a simple tri-diagonal system, *viz.*,

$$\mathbf{j}_k = \ {}^{-1}_{k}\mathbf{S}, \tag{9.44}$$

and then the $\bar{J}$ values are sums:

$$\bar{\mathbf{J}} = \sum_k w_k \ {}^{-1}_{k}\mathbf{S}. \tag{9.45}$$

In this way all the intensities can be eliminated from the system, which leaves the smaller system to solve, of which the order is $ND(NL + 2)$. The operation of inverting a tri-diagonal matrix is very efficient: $O(ND^2)$ operations, so the cost of eliminating the intensities is $O(NJ\,ND^2)$. The system that is left after the elimination is full, since the inverse of a tri-diagonal matrix is a full matrix. Thus the final solution of this system requires $O(ND^3(NL + 2)^3)$ operations. Rybicki's partitioning will be more efficient than the block-tri-diagonal scheme when $ND^2 < [(NJ + NL + 2)/(NL + 2)]^3$. Thus relatively few level populations and a large number of frequency–angle pairs favors Rybicki; comparable numbers of level populations and frequency–angle pairs favors the block tri-diagonal scheme. For the example dimensions above, the block-tri-diagonal scheme requires about $6.6 \times 10^{12}$ operations, while in Rybicki's scheme the elimination of the intensities takes $4 \times 10^7$ operations and the solution of the resulting system takes $1.4 \times 10^{11}$ operations. In this case the elimination cost is negligible, and the overall cost favors Rybicki by a factor 47.

The foregoing discussion describes solving the linear equations for the intensities themselves, but exactly the same reasoning also applies to the linear system that must be solved for each Newton–Raphson iteration; the sparsity pattern of the Jacobian matrix has the structure needed to apply Rybicki's elimination scheme. Auer (1984) gives quite a complete description of all the finite-difference methods, the different elimination schemes, and the organization of the complete linearization methods.

## 9.2 Partial redistribution

One important footnote to non-LTE line transfer concerns what is called *partial redistribution* or PRD, which was alluded to above. Spectral line transfer with partial frequency redistribution is treated well in Ivanov (1973) and Mihalas (1978). This is the subject of line scattering when there is some degree of correlation

between the frequency of absorption and the frequency of emission in the scattering process. Let us write the absorptivity as

$$k_\nu = k_L \phi(\nu), \tag{9.46}$$

then we write the emissivity, forgetting about the albedo for the moment, as

$$j_\nu = k_L \int_0^\infty d\nu' \, R(\nu, \nu') J_{\nu'}, \tag{9.47}$$

in which $R(\nu, \nu')$ is the *redistribution function*. The expression for the source function in this conservative scattering (albedo = 1) case is

$$S_\nu = \frac{1}{\phi(\nu)} \int_0^\infty d\nu' \, R(\nu, \nu') J_{\nu'}. \tag{9.48}$$

The redistribution function is the joint probability distribution of the two variables, $\nu$ and $\nu'$, the frequencies of emission and absorption. In order to conserve photons it must obey the relation

$$\int_0^\infty d\nu \, R(\nu, \nu') = \phi(\nu'). \tag{9.49}$$

Thermodynamic consistency also requires that it be symmetric in $\nu$ and $\nu'$:

$$R(\nu, \nu') = R(\nu', \nu) \tag{9.50}$$

apart from a small correction when $\nu - \nu_0$ and $\nu' - \nu_0$ are not negligible compared with $\nu_0$ and $kT/h$. If the frequencies are actually uncorrelated, then $R$ factors into a function of $\nu$ times a function of $\nu'$, which because of the last two constraints has to be $R = \phi(\nu)\phi(\nu')$. If this is put in, then the source function reduces to the frequency-independent value $\bar{J}$ that we used previously; this is then complete redistribution. The opposite approximation is that the frequency after scattering must be precisely the same as before, and in this case

$$R(\nu, \nu') = \phi(\nu)\delta(\nu' - \nu). \tag{9.51}$$

When the particular kinds of line broadening are considered, it is found that Doppler broadening corresponds to a mild, but nonzero correlation between the absorption and emission frequencies. Solutions taking the proper redistribution function into account show small differences from complete redistribution, which as a practical matter are ignored. Similarly if collisional line broadening is considered, either by ion microfields or electron impact, the redistribution function differs either very little or not at all from complete redistribution. The one case in which there are large differences between the accurate redistribution function and complete redistribution is resonance line scattering with a Lorentzian profile due to

natural broadening, perhaps combined with Doppler broadening. The term natural broadening refers to the Lorentzian broadening when the decay rate $\Gamma$ is due to the radiative decay alone, not to any collisional processes. In resonance line scattering the lower level of the line is a ground state, which lives a relatively long time between scattering events, and therefore its energy uncertainty is quite small. This means that in order to conserve energy the difference between the emitted photon energy and the absorbed photon energy will be of this order and therefore also small. Thus apart from Doppler broadening the frequency shift in the scattering is negligible. When this is combined with Doppler broadening the emission frequency can move in either direction relative to the absorption frequency by about one unit of $\Delta\nu_D$.

The definitive paper on the redistribution functions for the cases just discussed is Hummer (1962). He distinguishes four cases, of which three are the ones mentioned in the previous paragraph. These three are $R_I$, $R_{II}$, and $R_{III}$ in Hummer's notation. In $R_I$ the line is broadened solely by the Doppler effect, and redistribution is due to the difference of the atom's velocity as projected on the initial and final photon directions. In the frame of the atom the photon is absorbed and emitted precisely at the line center frequency. In $R_{II}$ there is a Lorentzian absorption profile in the frame of the atom, corresponding to natural broadening by the radiative decay of the excited state. It is supposed that the lifetime of the lower state is much longer, and conservation of energy ensures that the emitted and absorbed frequencies are the same in the frame of the atom. This model is appropriate for resonance lines. In the external frame the absorption profile becomes a Voigt function when Doppler broadening is added to the Lorentzian profile. If there is collisional broadening then the absorption profile in the frame of the atom is also Lorentzian, but the collisions cause the excited atom to lose memory of the initial frequency, and there is complete redistribution in the frame of the atom. When the Doppler effect is included the result is the $R_{III}$ redistribution function. Even though this is derived for complete redistribution in the frame of the atom, it is not quite complete redistribution in the external frame. Finally, Hummer considers a type of redistribution in which both the upper and lower states are broadened by radiative decay processes. With the inclusion of Doppler broadening this becomes $R_{IV}$. However, Hummer adopts a model from Heitler (1954) for the redistribution in the frame of the atom for this case, which turns out to be in error. The correct formula is in fact given by Weisskopf (1933) and by Wooley and Stibbs (1953). This was clarified by Omont, Smith, and Cooper (1972). Few results using $R_{IV}$ are available. The most rigorous development of the theory of the redistribution function, which relates the redistribution to the atomic kinetics and indicates precisely what mixture of $R_I$, $R_{II}$, $R_{III}$, and $R_{IV}$ is needed for each atomic transition, is by Cooper, Ballagh, Burnett, and Hummer (1982).

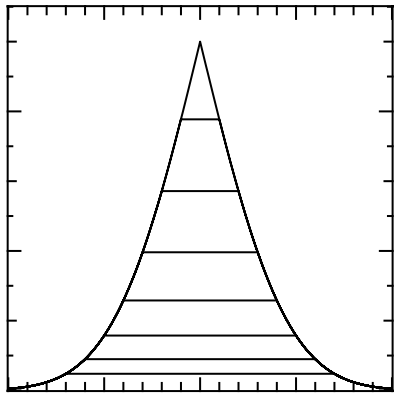

Fig. 9.2 The Doppler redistribution function $R_I\ (x, x')$ is plotted as a function of the scattered photon frequency displacement from line center, $x$, for values of the incoming photon frequency displacement from line center, $x'$, from 0 to 1.4 in steps of 0.2; $x$ and $x'$ are expressed in Doppler units.

The nature of $R_I$ is indicated in Figure 9.2. The region with $|x| < |x'|$ for a given $x'$ is rigorously flat; for $|x| > |x'|$ the function falls steeply. The probability of the emission frequency $x$ being near $\pm x'$ is greater with $R_I$ than with complete redistribution. However, $x$ and $x'$ are uncorrelated with this angle-averaged redistribution function. With angle-dependent redistribution $x$ and $x'$ are strongly correlated when $\mathbf{n}$ and $\mathbf{n}'$ are parallel, and strongly anti-correlated when $\mathbf{n}$ and $\mathbf{n}'$ are anti-parallel.

The nature of $R_{II}$ is qualitatively different, as seen in Figure 9.3. The accurate numerical evaluation of $R_{II}$ is somewhat troublesome; a good treatment is given by Adams, Hummer, and Rybicki (1971). While there is little correlation of $x$ and $x'$ in the Doppler core ($|x'| < 2$), in the Lorentzian wings $x$ and $x'$ become strongly correlated. In the far wings the asymptotic form of the marginal distribution is

$$\frac{1}{\phi(x')} R_{II}(x, x') \sim \text{ierfc}\left(\frac{1}{2}|x - x'|\right) \qquad \text{for } x' \gg 1, \tag{9.52}$$

where ierfc$(z)$ is the function defined by

$$\text{ierfc}(z) = \int_z^\infty \text{erfc}(t)\, dt = \frac{1}{\sqrt{\pi}}\, e^{-z^2} - z\, \text{erfc}(z). \tag{9.53}$$

The relative smallness of $|x - x'|$ in the line wings suggests that a Fokker–Planck treatment may be useful; this is done by Harrington (1973) with some success. A more thorough discussion is given by Frisch (1980). Frisch points out that $R_{IV}$ is like a weighted average of complete distribution with $R_{II}$, with the weight of

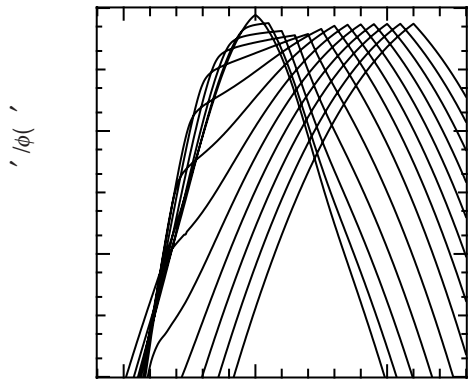

Fig. 9.3 The marginal distribution $R_{II}(x, x')/\phi(x')$ for the Voigt redistribution function for the case of coherence in the frame of the scattering atom is plotted as a function of the scattered photon frequency displacement from line center for values of the incoming photon frequency displacement from the line center, $x'$, from 0 to 4 in steps of 0.5. The Voigt parameter is 0.1.

complete redistribution being proportional to the natural width of the lower level and the weight of $R_{II}$ proportional to the natural width of the upper level. For most subordinate lines (with an excited state as the lower level) these widths are comparable, and thus so are the weights. In this case the complete redistribution part completely dominates the long-range behavior of the scattering problem. In other words, $R_{IV}$, like $R_I$ and $R_{III}$, behaves very much the same as complete redistribution. The odd man out is $R_{II}$, which is the realistic case for resonance-line scattering if the density is low enough that collisional broadening is negligible compared with natural broadening.

In the case of partial redistribution, the two-level-atom source function takes this form:

$$S_\nu \phi(\nu) = (1-\epsilon) \int_0^\infty d\nu' \, R(\nu, \nu') J_{\nu'} + \epsilon B_\nu \phi(\nu). \tag{9.54}$$

For complete redistribution, $S_\nu$ is independent of frequency and $R(\nu, \nu') = \phi(\nu)\phi(\nu')$, so a division by $\phi(\nu)$ recovers (9.8).

The problem of resonance line transfer in the situation described above, with quite large values of the optical thickness of the medium, leads to some interesting effects and has been well studied in the laboratory. Line photons in this kind of problem do a kind of double diffusion. The photons diffuse in real space while they simultaneously diffuse in frequency space. Of course the spatial diffusion coefficient is related to $1/\phi(\nu)$, so the diffusion in space is very rapid at frequencies that are far from line center. Since the photons must diffuse in frequency instead of

being independently sampled on every scattering, the effect is to keep them more confined toward line center in the partial redistribution case. This means that the typical mean free path is less, and that the photons will not travel as far in a given number of scatterings. Therefore the thermalization depth will be less for a given value of $\epsilon$. In fact it is found for scattering with partial redistribution as described that the thermalization length is roughly just the same as for a Doppler profile, while in complete redistribution, given the Lorentzian wings of the combined profile, the thermalization depth is much larger than that.

### 9.2.1 Asymptotic resonance line transfer with $R_{II}$

Harrington's (1973) asymptotic solution of the transfer equation for resonance line scattering with $R_{II}$ is useful for the insight it gives into the PRD transfer process. The action of the scattering kernel is approximated by expanding the function $J_{\nu'}$ inside the integral in a Taylor series about $\nu' = \nu$, then using the known moments of the $R_{II}$ function to obtain this result:

$$\frac{1}{\phi(x)}\int_{-\infty}^{\infty} dx' R_{II}(x,x')J(x')\,dx' \approx J(x) - \frac{1}{x}\frac{dJ(x)}{dx} + \frac{1}{2}\frac{d^2J(x)}{dx^2}, \quad (9.55)$$

so Milne's second equation, in the Eddington approximation, turns into

$$\frac{\partial^2 J}{\partial \tau^2} + \frac{3}{2}\phi^2(x)(1-\epsilon)\left[\frac{d^2J(x)}{dx^2} - \frac{2}{x}\frac{dJ(x)}{dx}\right] = 3\phi^2(x)\epsilon(J-B). \quad (9.56)$$

The optical depth scale $\tau$ is the mean over the line profile, given by $d\tau = k_L dz/\Delta\nu_D$. Two more transformations are introduced now. One is to notice that

$$\frac{3}{2}\phi^2(x)\left[\frac{d^2J(x)}{dx^2} - \frac{2}{x}\frac{dJ(x)}{dx}\right] \approx \frac{\partial^2 J}{\partial \sigma^2} \quad (9.57)$$

in terms of a new frequency-related variable $\sigma$ defined by

$$\sigma = \left(\frac{2}{3}\right)^{1/2}\int_0^x \frac{dx}{\phi(x)}. \quad (9.58)$$

The approximation is accurate in the Lorentzian wings of the Voigt profile, which is where all the transfer will take place in the asymptotic regime we want to consider. The variable $\sigma$ vanishes at line center, and in the wings $x \to \pm\infty$ it varies as $\sigma \sim \pm\sqrt{2/3}\pi|x|^3/(3a)$. We are also going to make the approximation $\epsilon \ll 1$ so the factor $1-\epsilon$ can be replaced by unity where it multiplies the frequency derivatives. We then have

$$\frac{\partial^2 J}{\partial \tau^2} + \frac{\partial^2 J}{\partial \sigma^2} = 3\phi^2\epsilon(J-B). \quad (9.59)$$

The second clever transformation is the result of observing that $\phi^2$, considered as a function of $\sigma$, is strongly peaked at $\sigma = 0$, much more so than $\phi$ is when considered as a function of $x$. So Harrington's second major approximation is to replace $3\phi^2$ by $\sqrt{6}\delta(\sigma)$. The factor $\sqrt{6}$ preserves the normalization of the profile. Thus finally the transfer equation becomes

$$\frac{\partial^2 J}{\partial \tau^2} + \frac{\partial^2 J}{\partial \sigma^2} = \sqrt{6}\epsilon(J - B)\delta(\sigma). \tag{9.60}$$

The delta function on the right-hand side tells us that line photons are created or destroyed entirely at line center. So except at line center, the intensity obeys a 2-D Laplace's equation in $\sigma$–$\tau$ space; in other words, there is double diffusion.

The solution $J(\tau, \sigma)$ of (9.60) should be continuous at line center, $\sigma = 0$, and in fact $J(\tau, 0)$ is the value of $\bar{J}$, which sets the population of the excited state. But there is a step discontinuity in $\partial J/\partial\sigma$:

$$\Delta\left(\frac{\partial J}{\partial \sigma}\right) = \sqrt{6}\epsilon[(J(\tau, 0) - B]). \tag{9.61}$$

Let us consider an infinite medium with a source $s$ of line photons confined to the sheet $\tau = 0$, in other words, $\epsilon B = s\delta(\tau)$. We take the Fourier transform of (9.60), using $\tilde{J}(k, \sigma) = \int d\tau\ \exp(ik\tau)J(\tau, \sigma)$. Then

$$-k^2\tilde{J} + \frac{\partial^2 \tilde{J}}{\partial \sigma^2} = \sqrt{6}\delta(\sigma)(\epsilon\tilde{J}(k, 0) - s). \tag{9.62}$$

The Fourier transform of the jump condition is

$$\Delta\left(\frac{\partial \tilde{J}}{\partial \sigma}\right) = \sqrt{6}(\epsilon\tilde{J}(k, 0) - s). \tag{9.63}$$

The solution must be of the form $\tilde{J} = A\exp(-|k\sigma|)$ with a suitable coefficient $A$. Putting this into the jump condition leads to

$$A = \frac{\sqrt{6}s}{2|k| + \sqrt{6}\epsilon}. \tag{9.64}$$

The inverse Fourier transform to obtain $J(\tau, \sigma)$ turns out after a little work to give

$$J(\tau, \sigma) = \sqrt{\frac{3}{2}}\frac{s}{\pi}\Re\left\{e^{\sqrt{3/2}(|\sigma| + i|\tau|)\epsilon}\, E_1[\sqrt{3/2}(|\sigma| + i|\tau|)\epsilon]\right\}. \tag{9.65}$$

The complex exponential integral function is tabulated in Abramowitz and Stegun (1964). We can see that the characteristic scale in $\tau$, and also in $\sigma$, is $1/\epsilon$, and thus the thermalization length scales in this way, just as it does for complete redistribution with Doppler broadening. Since the characteristic $\sigma$ also scales as $1/\epsilon$,

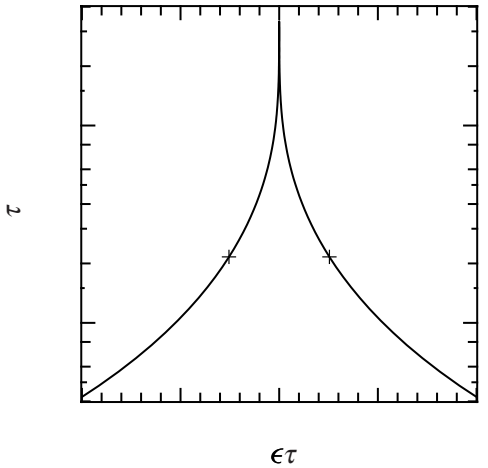


Fig. 9.4 The line-center mean intensity computed in Harrington's asymptotic model of PRD with $R_{II}$ is plotted as a function of $\epsilon\tau$. The crosses on the curve mark the edges of the region in $\tau$ that contains half the total population.

the characteristic frequency width in Doppler units is $x \sim (a/\epsilon)^{1/3}$. This asymptotic model is not applicable unless $x \gg 1$, so $\epsilon$ must be $\ll a$.

The spatial distribution of the excited state population is proportional to $J(\tau, 0)$, which can be expressed in terms of the auxiliary function for sine and cosine integrals $g(z)$ described by Abramowitz and Stegun (1964), Section 5.2:

$$J(\tau, 0) = \sqrt{\frac{3}{2}}\,\frac{s}{\pi}\,g\left(\sqrt{3/2}\epsilon\tau\right). \tag{9.66}$$

This distribution is shown in Figure 9.4. Half the excited atoms are contained in the interval $|\tau| < 0.509/\epsilon$, thus $0.509/\epsilon$ is the thermalization depth for small $\epsilon$.

Harrington's asymptotic theory is useful for aiding understanding, but as a numerical approximation it is not very good. It is based on the smallness of parameters like $(a\tau)^{-1/3}$ or $(\epsilon/a)^{1/3}$. The optical depth $\tau$ must be enormous, or $\epsilon$ tiny indeed, before the approximation starts to be accurate. For numerical results the calculations of Adams (1972) are much better.

## 9.3 Mean number of scatterings; mean path length

The mean number of scatterings and the mean path length are ways of describing the transfer of line radiation within a finite medium in an integral sense. There are reasonably accurate estimates available for these quantities, which makes them valuable for rough calculations. The references that develop the principal results for the mean number of scatterings are by Hummer (1964), Adams (1972), and

Ivanov (1973); the last is a general reference with many asymptotic expressions. Ivanov also discusses the mean path length.

The definition of the mean number of scatterings is the average over all photons created in a uniform distribution within the slab of the total number of times they interact with matter in the slab, counting the act of emission, before they either escape the medium or are quenched. The number of emissions is counted, but not a final quenching if there is one. This mean can be computed by counting the total number of emission events per unit time and dividing by the total number of creation events per unit time. This ratio is

$$\langle N \rangle = \frac{\int_0^{\tau_0} d\tau \int_0^{\infty} dx\, \phi(x) S(x,\tau)}{\int_0^{\tau_0} d\tau\, \epsilon B_\nu}, \tag{9.67}$$

in which $\tau_0$ is the full optical thickness of the slab. This simplifies for complete redistribution to

$$\langle N \rangle = \frac{\int_0^{\tau_0} d\tau\, S(\tau)}{\int_0^{\tau_0} d\tau\, \epsilon B_\nu}. \tag{9.68}$$

If the scattering albedo tends to zero, i.e. $\epsilon \to 1$, then $S$ becomes $\epsilon B_\nu$ and $\langle N \rangle = 1$. When $\epsilon$ is small compared with the escape probability $K_2(\tau)$ then the quenching probability is negligible and $\langle N \rangle$ tends to a limit that is independent of $\epsilon$ but depends on $\tau_0$. Hummer (1964) obtains an upper limit

$$\langle N \rangle \approx \frac{1}{\epsilon + (1-\epsilon) K_2(\tau_0/2)}, \tag{9.69}$$

which he proposes as an estimate. Ivanov's asymptotic methods for large $\tau_0$ sharpen up the estimate to the following, for the respective profile shapes:

$$\langle N \rangle \approx \begin{cases} \frac{1}{2}\tau_0 \sqrt{\ln(\tau_0/\sqrt{\pi})} & \text{Doppler} \\ \dfrac{\Gamma^2(1/4)}{(2\pi)^{3/2}} \sqrt{\dfrac{\tau_0}{a}} & \text{Voigt.} \\ \dfrac{\Gamma^2(1/4)}{(2\pi)^{3/2}} \sqrt{\tau_0} & \text{Lorentz.} \end{cases} \tag{9.70}$$

These estimates are half of Hummer (1964), for the Doppler case, and 21% less than Hummer's for the other two.

The mean number of scatterings in a finite slab in the conservative case $\epsilon = 0$ for PRD with $R_{II}$ is a quantity that is of prime interest. The numerical work by Adams (1972) and asymptotic analysis of Harrington (1973) both agree that the mean number of scatterings with $R_{II}$, for a photon source that is a thin sheet at the midplane of the slab, is proportional to $\tau_0$ in the asymptotic regime $(a\tau_0)^{1/3} \gg 1$.

Adams suggests a coefficient 0.75, but Harrington's expression

$$\langle N \rangle \sim 0.454658\tau_0 \tag{9.71}$$

fits Adams's numerical results about as well. The proportionality of $\langle N \rangle$ to $\tau_0$ rather than to $\sqrt{\tau_0/a}$ is a significant feature of ($R_{II}$) PRD; it is much harder to escape the medium with PRD. Harrington's result for a photon source uniformly distributed in the slab is similar, but with a coefficient of 0.332368 rather than 0.454658. This is the result that is comparable to the complete redistribution (CRD) expressions in the previous paragraph.

The mean path length of the scattering photon is defined as the average of the total distance it flies from the place where it is created to the place where it either is quenched or crosses the boundary of the medium. This is equal to the photon's dwelling time within the medium multiplied by the speed of light. The dwelling time can be calculated, in this steady-state problem, by dividing the total photon energy within the medium by the total energy rate of creating photons. This leads to

$$\langle \ell \rangle = \frac{\Delta\nu_D}{k_L} \frac{\int_0^{\tau_0} d\tau \int_0^{\infty} dx\, J(x,\tau)}{\int_0^{\tau_0} d\tau\, \epsilon B_\nu}. \tag{9.72}$$

The integrals for $\langle N \rangle$ and $\langle \ell \rangle$ are very similar; in fact, for a square profile there is the simple relation

$$(1-\epsilon)\langle \ell \rangle = \frac{\Delta\nu_D}{k_L}(\langle N \rangle - 1). \tag{9.73}$$

This says that the average flight path is the mean free path $\Delta\nu_D/k_L$. (Remember that the number of flights is one less than the number of scatterings by the definition we are using.)

Ivanov's (1973) results for the mean path length for $\epsilon = 0$ and $\tau_0 \gg 1$ are the following:

$$\langle \ell \rangle \sim \frac{\Delta\nu_D}{k_L} \times \begin{cases} \tau_0\sqrt{\ln(\tau_0/\sqrt{\pi})} & \text{Doppler} \\ \dfrac{9}{4}\,\tau_0 & \text{Voigt or Lorentz} \end{cases} \tag{9.74}$$

In PRD, with $R_{II}$, and with a uniformly distributed photon source in the slab, Harrington's methods lead to a value of the mean path length given by

$$\langle \ell \rangle \sim \frac{\Delta\nu_D}{k_L} 0.692739\,(a\tau_0^4)^{1/3}. \tag{9.75}$$

This exceeds the thickness of the slab by a factor that is $O((a\tau_0)^{1/3})$. The accumulated smaller flights amount to much more than the single longest flight in this case.

If there is both a nonzero quenching probability $\epsilon$ and a continuous absorption coefficient $k_c$, then Ivanov (1973), Section 8.10, points out that the mean escape probability is $1 - \epsilon\langle N\rangle - k_c\langle\ell\rangle$. This is physically obvious once it is recognized that the events of escape, quenching, and continuous absorption all remove the photons, are mutually exclusive, and exhaust all the possible photon fates. The discussion of mean escape probabilities leads directly to the topic of Irons's theorem.

### *9.3.1 Irons's theorem*

Irons's theorem says that the Net Radiative Bracket is equal to the single-flight escape probability in the mean, with the mean defined using a weighting function equal to the emissivity. A good discussion of Irons's theorem, and of escape probability matters in general, is given by Rybicki (1984). The following is a demonstration of this for the plane-parallel slab (optical thickness $\tau_0$) with complete redistribution but no continuous absorption. The transfer equation is

$$\mu \frac{dI_x(\tau, \mu)}{d\tau} = \phi(x)[I_x(\tau, \mu) - S(\tau)]. \tag{9.76}$$

The intensity that emerges at $\tau = 0$ with $\mu > 0$ is given by

$$I_x(0, \mu) = \int_0^{\tau_0} \frac{d\tau}{\mu} S(\tau) \exp\left[-\frac{\tau\phi(x)}{\mu}\right]. \tag{9.77}$$

But an integration of the transfer equation directly, and noting that $I_x(\tau_0, \mu) = 0$ for $\mu > 0$, leads to

$$I_x(0, \mu) = -\int_0^{\tau_0} \frac{d\tau}{\mu} \phi(x)[I_x(\tau, \mu) - S(\tau)]. \tag{9.78}$$

Then we can replace $\mu$ with $-\mu$ and develop two expressions for $I_x(\tau_0, -\mu)$:

$$I_x(\tau_0, -\mu) = \int_0^{\tau_0} \frac{d\tau}{\mu} S(\tau) \exp\left[-\frac{(\tau_0 - \tau)\phi(x)}{\mu}\right] \tag{9.79}$$

and

$$I_x(\tau_0, -\mu) = \int_0^{\tau_0} \frac{d\tau}{-\mu} \phi(x)[I_x(\tau, -\mu) - S(\tau)]. \tag{9.80}$$

Now we equate the two expressions for $I_x(0, \mu)$, and also the two expressions for $I_x(\tau_0, -\mu)$, and average those equations. This yields

$$\int_0^{\tau_0} \frac{d\tau}{\mu}\phi(x)\frac{1}{2}\left\{\exp\left[-\frac{\tau\phi(x)}{\mu}\right] + \exp\left[-\frac{(\tau_0-\tau)\phi(x)}{\mu}\right]\right\} S(\tau)$$
$$= \int_0^{\tau_0} \frac{d\tau}{\mu}\phi(x)S(\tau)\left[1 - \frac{j_x(\tau,\mu)}{S(\tau)}\right]. \tag{9.81}$$

The quantity $j_x(\tau, \mu)$ is the Feautrier average of the intensity at $\pm\mu$. The next step is to multiply this equation by $\mu$ and integrate over all $x$ and over the range $[0, 1]$ of $\mu$. The result is

$$\int_0^{\tau_0} d\tau\, S(\tau)\frac{1}{2}\left[K_2(\tau) + K_2(\tau_0-\tau)\right] = \int_0^{\tau_0} d\tau\, S(\tau)\left[1 - \frac{\bar{J}(\tau)}{S(\tau)}\right]. \tag{9.82}$$

This is a statement of Irons's theorem for this case, since $z = 1 - \bar{J}/S$ is the Net Radiative Bracket and the combination $p_{\rm esc} = \frac{1}{2}\left[K_2(\tau) + K_2(\tau_0 - \tau)\right]$ is the two-sided escape probability for the finite slab, generalizing (9.20). It is fairly clear from this derivation, and from Rybicki's (1984) presentation, that this result can be extended to arbitrary geometries. An immediate corollary that Rybicki draws is the relation between the mean number of scatterings and the escape probability that appears in Irons's theorem. It is

$$\langle N\rangle = \frac{1}{\epsilon + (1-\epsilon)\langle z\rangle} = \frac{1}{\epsilon + (1-\epsilon)\langle p_{\rm esc}\rangle}. \tag{9.83}$$

The first equality is an identity based on the definition of $z = 1 - \bar{J}/S$, and the second equality is Irons's theorem. This relation between the mean number of scatterings and the single-flight escape probability recalls Hummer's relation (9.69). In Hummer's relation the value of $p_{\rm esc}$ at the center of the slab appears instead of the source-function-weighted average over the slab.

## 9.4 Time-dependent line transport

Our discussion so far has concerned only steady-state line transfer. Now we want to consider the time-dependent effects. Mostly this will be concerned with learning what the important time scales are; doing time-dependent practical problems is a major computational effort not a pedagogical topic.

First we need to consider the two causes of time dependence in spectral line transport: (1) the spontaneous lifetime $t_{\rm sp} = 1/A_{u\ell}$, which causes the source function to lag the radiative and collisional rates by a time of order $t_{\rm sp}$; and (2) the time of flight $\lambda_{\rm mfp}/c$ for a mean free path, which causes the mean intensity and the photoexcitation rates to lag the source function in time by about $\lambda_{\rm mfp}/c$. The quantities

vary by orders of magnitude in different radiation environments, and therefore so does their ratio. The spontaneous lifetime varies less than the flight time; its order of magnitude is

$$t_{\rm sp} \approx \frac{23}{(h\nu/{\rm eV})^2}\ {\rm ns}. \tag{9.84}$$

This is for a line with unit oscillator strength, and $h\nu/{\rm eV}$ is the line energy in electron volts. We see that this time scale is very short in astrophysical terms, when the line energy is indeed around 1 eV, and it is even shorter for high-energy environments when the line is in the keV x-ray range. The flight time of the line photon is harder to estimate in general terms. In many problems of stellar astrophysics the mean free path is of the order of an atmospheric scale height down to a small fraction of a scale height. The flight time for a scale height in the solar photosphere is 0.4 ms. This is four orders of magnitude greater than the spontaneous lifetime. Thus when the time scale is large enough to be of any interest in the astrophysical problem, the flight time will greatly exceed the spontaneous lifetime.

In problems that are on a terrestrial scale, with dimensions from microns (laser targets) up to meters (laboratory scale), the time of flight will range from less than a femtosecond up to a few nanoseconds. In essentially all of these cases the time of flight will be much less than the spontaneous lifetime. Thus in most laboratory-scale problems the dominant time dependence comes from the spontaneous lifetime, while in astrophysical problems the dominant time scale is the flight time.

The time dependence associated with the spontaneous lifetime – in general with the finiteness of all the rates – is incorporated in the two-level-atom model by using the rate for the excited-state population in place of the state–state equation. Thus

$$\frac{dN_u}{dt} = N_\ell(B_{\ell u}\bar{J} + N_{\ell u}) - N_u(A_{u\ell} + B_{u\ell} + C_{u\ell}). \tag{9.85}$$

The important applications of time-dependent transport are to resonance lines, so in that case the time dependence of the lower-level population is neglected. Using (9.85) and the definition of the source function leads to

$$\frac{dS}{dt} = A_{u\ell}\left(1 + \frac{g_\ell + g_u}{g_u}\frac{S}{2h\nu^3/c^2}\right)\left[\bar{J} + \epsilon' B - (1+\epsilon')S\right]. \tag{9.86}$$

The stimulation factor $1 + [(g_\ell + g_u)/g_u]2h\nu^3/c^2$ can normally be omitted, leaving this useful equation:

$$\frac{dS}{dt} = A_{u\ell}\left[\bar{J} + \epsilon B - (1+\epsilon)S\right]. \tag{9.87}$$

In the following discussion we will first consider an example in which flight time is dominant and the spontaneous lifetime is neglected, and then one in which

the reverse occurs. Let us return to the time-dependent transport equation for a line formed by a two-level atom with partial redistribution, and we will also include a background continuous opacity. The equation including time of flight is

$$\frac{1}{c}\frac{\partial I_\nu}{\partial t} + \mathbf{n}\cdot\nabla I_\nu = -(k_L\phi(\nu) + k_c)I_\nu + (1-\epsilon)k_L\int d\nu' R(\nu,\nu')J_{\nu'} + \epsilon B\phi(\nu) + k_c S_c. \tag{9.88}$$

Now we form the Laplace transform, with $\tilde{I}_\nu(p) = \int_0^\infty dt\ \exp(-pt)I_\nu(t)$. The equation becomes

$$\mathbf{n}\cdot\nabla\tilde{I}_\nu = -\left[k_L\phi(\nu) + k_c + \frac{p}{c}\right]\tilde{I}_\nu + (1-\epsilon)k_L\int d\nu' R(\nu,\nu')\tilde{J}_{\nu'} + \frac{1}{p}\epsilon B\phi(\nu) + \frac{1}{p}k_c S_c + \frac{1}{c}I_\nu(0). \tag{9.89}$$

What we notice about this equation is that it is identical to a steady-state line transfer equation with an extra contribution $p/c$ in the continuous opacity, an effective continuous emissivity of $k_c S_c/p + I_\nu(0)/c$, and an effective Planck function of $B/p$.

We want to find out about the rate at which the intensity relaxes toward a steady state, assuming there is one. The steady-state intensity obeys this equation

$$\mathbf{n}\cdot\nabla I^s_\nu = -[k_L\phi(\nu) + k_c]I^s_\nu + (1-\epsilon)K_L\int d\nu' R(\nu,\nu')J^s_{\nu'} + \epsilon B\phi(\nu) + k_c S_c. \tag{9.90}$$

If we define $\Delta I_\nu$ to be $I_\nu - I^s_\nu$, then its Laplace transform obeys this equation

$$\mathbf{n}\cdot\nabla(\Delta\tilde{I}_\nu) = -\left[k_L\phi(\nu) + k_c + \frac{p}{c}\right]\Delta\tilde{I}_\nu + (1-\epsilon)k_L\int d\nu' R(\nu,\nu')\Delta\tilde{J}_\nu + \frac{1}{c}\Delta I_\nu(0). \tag{9.91}$$

A theorem on Laplace transforms tells us what the effect is of $k_c$ on the time dependence: if $(\Delta I_\nu)_0(t)$ is the solution without continuous absorption, then $\exp(-k_c ct)(\Delta I_\nu)_0(t)$ is the solution including continuous absorption. So we can drop $k_c$ at this point with no loss of generality, since it can always be put back later using this result.

Let us consider the case of complete redistribution in an infinite homogeneous medium with an initially white, isotropic departure $\Delta I_\nu(0)$ from the steady-state intensity. For convenience we convert the frequencies to Doppler units, and use the line profile function on the Doppler-width scale $\phi(x)$, and define a new variable $\beta = p\Delta\nu_D/(k_L c)$. The redistribution function becomes $R(x,x') = \phi(x)\phi(x')$.

The transform then obeys this equation

$$\Delta\tilde{I}_x[(\phi(x)+\beta] = (1-\epsilon)\phi(x)\tilde{\bar{J}} + \frac{\Delta\nu_D}{k_L c}\Delta I_\nu(0). \tag{9.92}$$

Multiplying this equation by $\phi(x)/[\phi(x)+\beta]$ and integrating over $x$ leads to

$$\tilde{\bar{J}} = (1-\epsilon)\tilde{\bar{J}}\int_{-\infty}^{\infty} dx\,\frac{\phi^2(x)}{\phi(x)+\beta} + \frac{\Delta\nu_D}{k_L c}\Delta I_\nu(0)\int_{-\infty}^{\infty} dx\,\frac{\phi(x)}{\phi(x)+\beta}. \tag{9.93}$$

A function $F(\beta)$ that depends on the shape of the line profile, often called the curve-of-growth function, is defined by

$$F(\beta) = \int_{-\infty}^{\infty} dx\,\frac{\phi(x)}{\phi(x)+\beta}. \tag{9.94}$$

The first integral in (9.93) is seen to be $1-\beta F(\beta)$. Therefore the solution of (9.93) is

$$\tilde{\bar{J}} = \frac{\Delta\nu_D\Delta I_\nu(0)}{k_L c}\frac{F(\beta)}{\epsilon+(1-\epsilon)\beta F(\beta)}. \tag{9.95}$$

Our task now is to consider specific shapes of the line profile function, approximate $F(\beta)$ for each of these for $\beta \to 0$, and then, since $\beta \propto p$, use the approximation to get the inverse Laplace transform, and thereby find $\bar{J}$ for large $t$. For a square line profile, i.e., a "line" that has a constant opacity rather than a smooth shape, we use $\phi(x) = 1$ for $0 \le x \le 1$, with the result that $F(\beta) = 1/(1+\beta)$. Then we see that

$$\tilde{\bar{J}} = \frac{\Delta\nu_D\Delta I_\nu(0)}{k_L c}\frac{1}{\epsilon+\beta} = \Delta I_\nu(0)\frac{1}{p+\epsilon k_L c/\Delta\nu_D}. \tag{9.96}$$

The inverse Laplace transform gives $\bar{J} = \Delta I_\nu(0)\exp(-\epsilon k_L c t/\Delta\nu_D)$. In other words, the initial departure of the intensity from the steady-state value decays with a mean lifetime given by the time to make $1/\epsilon$ flights with a mean free path of $\Delta\nu_D/k_L$.

With Doppler broadening the curve of growth function turns out to be

$$F(\beta) \sim 2\sqrt{\ln\left(\frac{1}{\sqrt{\pi}\beta}\right)}, \tag{9.97}$$

when $\beta$ is small. We will refer to the $\sqrt{\ln}$ expression as $C(\beta)$; it is a slowly-varying function, ranging from 1 to 3 over quite a large range in $\beta$. The transform of $\bar{J}$ can then be written as

$$\tilde{\bar{J}} \sim \frac{\Delta\nu_D\Delta I_\nu(0)}{k_L c}\frac{2C(\beta)}{\epsilon+(1-\epsilon)p\Delta\nu_D 2C(\beta)/(k_L c)}. \tag{9.98}$$

In the Laplace inversion, most of the contribution comes from values of $p$ that make $\beta \approx \epsilon$. Making this substitution in $C(\beta)$ leads to

$$\bar{J} \sim \Delta I_\nu(0) \exp\left(-\frac{\epsilon k_L c t}{\Delta\nu_D 2C(\epsilon)}\right). \tag{9.99}$$

This is almost the same result, with the same mean decay time, as for the square profile, except that the mean free path and the mean free time are increased by the factor $2C(\epsilon)$.

For a Voigt profile it is sufficient to calculate $F(\beta)$ using the large-$x$ asymptotic form of the profile, $\phi(x) \sim a/(\pi x^2)$. Then it is easy to see that $F(\beta) \sim \sqrt{\pi a/\beta}$. This will only apply for $\beta \ll a$. Then the transform is

$$\tilde{\bar{J}} \sim \frac{\Delta\nu_D \Delta I_\nu(0)}{k_L c} \frac{\sqrt{\pi a/\beta}}{\epsilon + \sqrt{\pi a \beta}} = \Delta I_\nu(0) \frac{1}{\sqrt{p}[\sqrt{p} + \epsilon\sqrt{k_L c/(\pi \Delta\nu_D a)}]}. \tag{9.100}$$

Finding the inverse Laplace transform in the tables leads to

$$\bar{J} \sim \Delta I_\nu(0) \exp\left(\frac{\epsilon^2 k_L c t}{\pi \Delta\nu_D a}\right) \operatorname{erfc}\left(\epsilon\sqrt{\frac{k_L c t}{\pi \Delta\nu_D a}}\right). \tag{9.101}$$

In this case the decay time is of order $a/\epsilon^2$ times the flight time for a line-center mean free path.

In every case, the mean decay time is about equal to the flight time for the thermalization length corresponding to the given profile and value of $\epsilon$. This is at first surprising since the flight time adds up all the flight distances rather than taking the net displacement. But we recall the longest-single-flight picture, which says that the sum of all the flights is just about the same as the longest one, and also about the same as the net displacement.

There are other cases to consider, such as PRD, and other problems to analyze, such as the time-dependent spreading of line radiation in an infinite medium with no quenching or absorption. We will round out the present discussion by treating that problem with CRD in the case that the spontaneous lifetime dominates the time dependence rather than the flight time.

The dynamical equation for the source function becomes

$$\frac{\partial S(\tau, t)}{\partial t} = A_{ul}\left[\int_{-\infty}^{\infty} d\tau'\, K_1(\tau - \tau') S(\tau') - S(\tau)\right]. \tag{9.102}$$

This becomes Holstein's (1947a,b) and Biberman's (1947) integro-differential equation for trapped resonance-line radiation when we recognize that $S$ is proportional to the excited-state population. We suppose that at $t = 0$ there is a thin

sheet of excited atoms at $\tau = 0$. We Fourier analyze this equation with respect to $\tau$ and obtain

$$\frac{\partial \tilde{S}}{\partial t} = A_{u\ell}[\tilde{K}_1(k) - 1]\tilde{S}. \tag{9.103}$$

At the initial time the Fourier transform of the delta function representing the sheet of excitation is $\tilde{S}(0) = 1$. And therefore the solution for the transform is

$$\tilde{S}(k, t) = \exp\left\{-A_{u\ell}[1 - \tilde{K}_1(k)]t\right\}. \tag{9.104}$$

In order to find how $S(t)$ varies with large $t$ we have to investigate $\tilde{K}_1(k)$ for $k \to 0$. This is the work done by Ivanov and coworkers and reported in Ivanov (1973). The general expression is

$$\tilde{K}_1(k) = \int_{-\infty}^{\infty} dx\, \frac{\phi^2(x)}{k} \tan^{-1} \frac{k}{\phi(x)}. \tag{9.105}$$

The results obtained from the asymptotic evaluation of the integral are:

$$\tilde{K}_1(k) \sim \begin{cases} 1 - \dfrac{\pi}{4} \dfrac{|k|}{\sqrt{\ln(1/(\sqrt{\pi}|k|))}} & \text{Doppler} \\ 1 - \dfrac{\sqrt{2\pi a|k|}}{3} & \text{Voigt.} \\ 1 - \dfrac{\sqrt{2\pi|k|}}{3} & \text{Lorentz} \end{cases} \tag{9.106}$$

The inversion to find $S(\tau, t)$ then gives in the Doppler case

$$S(\tau, t) \sim \frac{W}{\pi} \frac{1}{\tau^2 + W^2}, \tag{9.107}$$

in which $W$ is a Lorentzian width in optical depth given by

$$W = \frac{\pi A_{u\ell} t}{4\sqrt{\ln(A_{u\ell} t/\sqrt{\pi})}}. \tag{9.108}$$

The wave of excited atoms spreads linearly in time with an effective velocity

$$\frac{W\lambda_{\text{mfp}}}{t} = \frac{\pi A_{u\ell}\lambda_{\text{mfp}}}{4\sqrt{\ln(A_{u\ell} t/\sqrt{\pi})}}. \tag{9.109}$$

This is guaranteed to be small compared with $c$ since the lifetime dominates the time of flight only if $A_{u\ell}\lambda_{\text{mfp}} \ll c$.

In the Voigt case the form for $S(\tau, t)$ at large $t$ is

$$S(\tau, t) \sim \frac{9}{(A_{u\ell} t)^3} z^3 g_F(z), \tag{9.110}$$

in terms of the variable $z = A_{u\ell}t/(3\sqrt{\tau})$ and the function $g_F(z)$ (not the same as the earlier $g(z)$) that is related to the Fresnel integrals, see Abramowitz and Stegun (1964), Section 7.3, (7.3.6). The range of $\tau$ that contains half the excited atoms is found to be $|\tau| \leq 0.86(A_{u\ell}t)^2$. Remarkably, the wave of excited atoms spreads at an accelerated rate as time goes on! The effective wave speed is of order $A_{u\ell}^2\lambda_{\rm mfp}t$, which is $A_{u\ell}t$ times larger than in the Doppler case. Thus after several scatterings the Voigt wave of excited atoms is moving much faster than the Doppler one. This model is only for CRD; with PRD the spread of excited atoms is significantly slower. We can estimate the mean number of scatterings by $N \approx A_{u\ell}t$. Then the width of the excited atom distribution would be approximately the thickness of the finite slab that would have that mean number of scatterings, in other words, $\tau \approx N \approx A_{u\ell}t$. This corresponds to the same wave speed as in the Doppler case.

Holstein (1947b) treats the homogeneous infinitely long cylinder in a calculation that was extended by Payne and Cook (1970). These authors were seeking the decay constant eigenvalue for the bounded medium; Payne and Cook also provide the spatial variation of $S$ for large time. The scaling of characteristic size with time agrees with the results above; the shape functions are modified for cylindrical geometry vs slab geometry.